Two Cation Disulfide Layers in the $W_xMo_{(1−x)}S_2$ Lamellar Solid Solution

Cécile Thomazeau,* Christophe Geantet,* Michel Lacroix,* Virginie Harlé,† Simone Benazeth,‡ Christiane Marhic,§ and Michel Danot§

*Institut de Recherches sur la Catalyse, UPR CNRS 5401, 2 Avenue Albert Einstein, 69626 Villeurbanne cedex, France; †Institut Français du Pétrole, 1–4 avenue de Bois-Préau, 92852 Rueil-Malmaison cedex, France; ‡Laboratoire pour l'Utilisation du Rayonnement Electromagnétique, UMR 130, CNRS–Université Paris Sud (Paris XI), bat. 209 D, BP 34, 91898 Orsay cedex, France; and §Institut des Matériaux Jean Rouxel, UMR 6502, CNRS–Université de Nantes, 2 Rue de la Houssinière, BP 32229, 44322 Nantes cedex 3, France

E-mail: michel.danot@cnrs-imn.fr

$W_xMo_{(1−x)}S_2$ compounds with both molybdenum and tungsten present in every disulfide layer, i.e., as an intralayer solid solution, can be obtained. Several synthesis routes have been used but all of them do not allow this solid solution, which evidences the decisive role of the nature of the precursor, to be obtained. We never observed formation of a $W_xMo_{(1−x)}S_2$ solid solution resulting from stacking of homocationic [WS_2] and [MoS_2] layers (interlayer solid solution). © 2001 Academic Press

*Key Words:* molybdenum disulfide; tungsten disulfide; solid solution; EXAFS.

I. INTRODUCTION

In MS_2 lamellar transition metal disulfides, the layer is constituted by three hexagonal atomic planes, a cationic one "sandwiched" by two anionic ones. Within the layer, every M atom is surrounded by a sulfur octahedron (M = Ti, for instance) or a sulfur trigonal prism (M = Mo or W for instance) with a coordination number of 6 in both cases. The crystals result from the stacking of such layers along the c axis according to the scheme $[S–M–S]_\infty$. Different stacking sequences exist, leading to various structures that are designated as 1T (one layer per unit cell, trigonal symmetry), 2H (two layers per unit cell, hexagonal symmetry), 3R (three layers per unit cell, rhombohedral symmetry), etc. (1). The anisotropy of such structures results from the coexistence of strong iono-covalent metal–sulfur bonds within the S–M–S layer and of weak bonds between adjacent layers (these weak bonds correspond to the interlayer space known as the van der Waals gap). This particular arrangement explains the extensive work devoted to these systems with regards to their synthesis, properties, and applications as catalysts (2), lubricating agents (3), or host compounds for the intercalation of various species (4).

By contrast, only sparse literature data concerning the synthesis of solid solutions such as $M^a_xM^b_{(1−x)}S_2$ were reported, even if the M^aS_2 and M^bS_2 sulfides both crystallize with the same site geometry (octahedron or trigonal prism). Such a solid solution was evidenced for the Nb–Mo disulfide system (5, 6) and proposed for the Mo–W one (7, 8). However, the atomic arrangement was determined only in the first case (6). The present work was undertaken in order to determine the structural characteristics of a possible $W_xMo_{(1−x)}S_2$ solid solution for reasons that will be indicated in the following section.

II. WHICH STRUCTURE FOR AN $M^a_xM^b_{(1−x)}S_2$ SOLID SOLUTION?

Two structural models may be envisioned for a $M^a_xM^b_{(1−x)}S_2$ layered solid solution: (i) every layer could contain only one type of cation, the phase resulting from the stacking of homocationic [M^aS_2] and [M^bS_2] layers (interlayer solid solution), or (ii) the two cations could be present in every layer, the phase resulting from the stacking of heterocationic [$M^a_xM^b_{(1−x)}S_2$] layers (intralayer solid solution). In both cases, the Vegard's law should be obeyed, at least approximately. However, except for ordered arrangements for which superstructure reflections would provide valuable information, the position of the diffraction lines cannot make it possible to distinguish between the two models due to the statistical character of the X-ray diffraction technique, and only local methods, such as EXAFS for instance, may provide relevant information. In a lamellar disulfide, the Fourier transform of the EXAFS spectrum recorded at the cation edge exhibits two intense peaks, the first one corresponding to the first sulfur neighbors of the absorbing cation and the second to its first in-plane cationic environment (Fig. 1) without any multiple-scattering
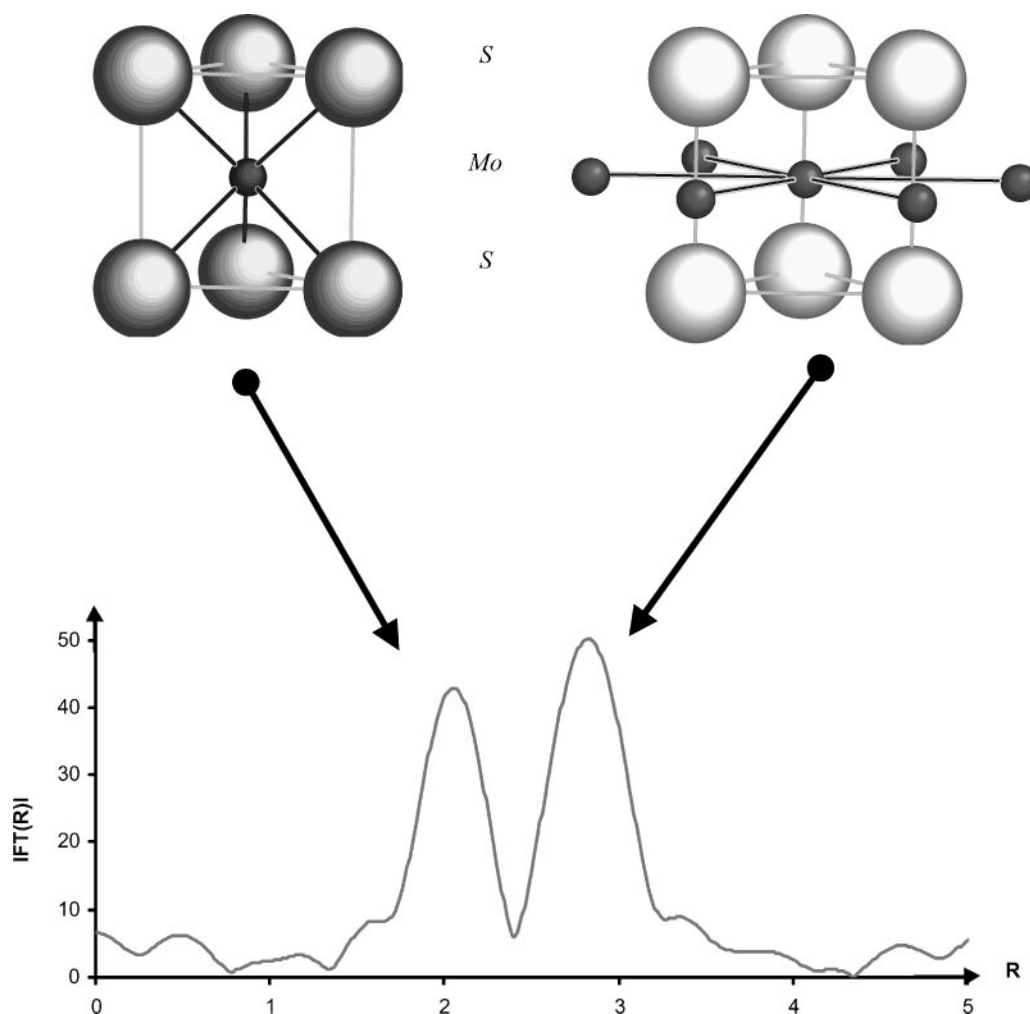
FIG. 1. Fourier transform obtained at the Mo K-edge for MoS_2: the first peak corresponds to the first sulfur neighbors of molybdenum, the second peak to its first in-plane cationic environment.

contribution (9). Consequently, for an interlayer solid solution, the M^a cation would "see" only M^a cationic neighbors and the M^b cation only M^b cationic neighbors, just as in their own M^aS_2 and M^bS_2 disulfides, while for an intralayer solid solution the M^a cations and the M^b cations would "see" both M^a and M^b neighbors. Therefore EXAFS is a powerful technique for discriminating between the two possibilities. This was fairly illustrated in the case of the $Nb_xMo_{(1-x)}S_2$ compounds: cell-parameter evolution versus composition (x) showed that this system is effectively a solid solution (5), and EXAFS results evidenced the presence of both Nb and Mo cations in every $[MS_2]$ layer (6) according to the intralayer solid solution model.

The in-plane periodicity is significantly different for $[NbS_2]$ and $[MoS_2]$ layers ($a_{NbS_2} = 3.330\,\text{Å}$ and $a_{MoS_2} = 3.161\,\text{Å}$). For this reason, the stacking of alternate homocationic $[NbS_2]$ and $[MoS_2]$ layers (interlayer solid solution) would induce important distortions (and strains) in order to adapt both types of layers to a common a

periodicity, another possibility being the formation of an uncommensurate misfit arrangement, with noticeable strains too. In the case of the the $Nb_xMo_{(1-x)}S_2$ system, the observed intralayer model thus appears energetically more favorable since it allows "dilution" of the strains.

The Mo–W disulfide system also seems propitious for the obtention of a solid solution since MoS_2 and WS_2 (10–12) are isostructural, with the same sulfur coordination geometry of the cation (trigonal prismatic), the same space group ($P6_3/mmc$), and the same stacking sequence (2H). Moreover, in contrast to the Nb–Mo system, the a cell parameters of the WS_2 and MoS_2 partners are nearly identical ($a_{MoS_2} = 3.161\,\text{Å}$ and $a_{WS_2} = 3.154\,\text{Å}$) (13). For this reason, packing of alternate homocationic $[WS_2]$ and $[MoS_2]$ layers can be expected to be possible without noticeable distortions (and strains) being induced. From this point of view, the $W_xMo_{(1-x)}S_2$ system appears ideal for obtaining an interlayer solid solution, at least for particular compositions

($x = 0.50$ for instance), that could allow simple ordered arrangements along the c axis. Our study of the $W_xMo_{(1-x)}S_2$ system aimed to determine whether this geometrical factor is determinant concerning the nature of a lamellar disulfide solid solution. Lastly it is to be noted that the Mo–W disulfide system is very favorable for EXAFS identification of a possible solid solution because backscattering amplitudes and phases are very different for molybdenum and tungsten.

III. EXPERIMENTAL

III.1. Synthesis

$W_xMo_{(1-x)}S_2$ compounds were prepared using the ammonium tetrathiomolybdate $(NH_4)_2MoS_4$ and ammonium tetrathiotungstate $(NH_4)_2WS_4$ salt precursors. Ammonium tetrathiomolybdate was prepared according to the procedure previously described (14). This method consists of dissolving at room temperature commercial ammonium heptamolybdate $(NH_4)_6Mo_7O_{24}, 4H_2O$ (40 g) in 400 mL of an aqueous solution of $(NH_4)_2S$ (20%). After one week, red crystals formed and grew. They were isolated by filtration, rinsed with acetone, and dried under vacuum. Chemical analysis agreed with the expected $(NH_4)_2MoS_4$ formula. An UV-Vis spectrum of diluted solution of this compound only exhibited intense absorption bands at 470, 318, and 242 nm. According to Diemann and Müller (15), this is the signature of pure $(NH_4)_2MoS_4$ since the presence of residual oxothiomolybdate species would give rise to several other bands. Ammonium tetrathiotungstate was prepared using the method described in the literature (16, 17). Forty grams of ammonium dodecatungstate $(NH_4)_{10}W_{12}O_{41}, 14H_2O$ were dissolved in 200 mL of a 1.75 M aqueous solution of NH_3. The solution was then kept for 4 h under H_2S bubbling at 333 K and then cooled and maintained at 273 K overnight. A precipitate of orange–yellow $(NH_4)_2WS_4$ crystals was isolated by filtration, rinsed with acetone, and dried under vacuum. As for the Mo precursor, chemical analysis and UV-Vis spectroscopy confirm the synthesis of pure $(NH_4)_2WS_4$.

$(NH_4)_2WS_4$ and $(NH_4)_2MoS_4$, taken in various proportions, were then dissolved in water, and then the solution dried under vacuum. X-ray diffraction patterns did not make it possible to identify unambiguously the resulting solids as $(NH_4)_2W_xMo_{(1-x)}S_4$ solid solution or a two-phase system due to the similarity of the cell parameters of $(NH_4)_2WS_4$ and $(NH_4)_2MoS_4$ (18, 19). However, for the equimolar composition, a very weak line attributable to the 001 reflection could be detected. This line, forbidden by the space group of $(NH_4)_2WS_4$ and $(NH_4)_2MoS_4$ (Pnma (18, 19)), could be the signature of a solid solution with ordered arrangement of the W and Mo cations. Nevertheless, considering its weakness, this line alone cannot be considered as a proof of the ordering, and
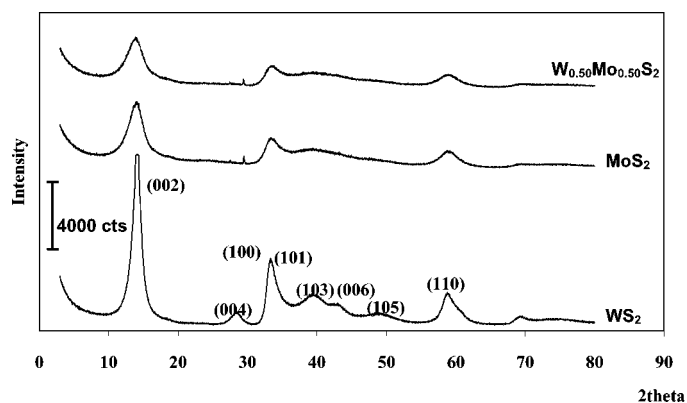

FIG. 2. X-ray diffraction patterns of WS_2, MoS_2, and $W_{0.50}Mo_{0.50}S_2$ prepared at 673 K by treatment, under H_2S flow, of respectively ammonium tetrathiotungstate, ammonium tetrathiomolybdate, and the product of cocrystallization of these two thiosalts.

consequently of the existence of a solid solution. We also tried to identify the cocrystallization products by EXAFS measurements: in the case of a two-phase system, the cationic neighbors of Mo would be uniquely Mo and those of W uniquely W; in the case of a solid solution, Mo and W would have both Mo and W neighbors. Unfortunately, due to the large interatomic distance (> 6 Å), the corresponding peak could not be detected. Whatever their nature, solid solution or intimate mixture of $(NH_4)_2WS_4$ and $(NH_4)_2MoS_4$, the solids resulting from this cocrystallization were then heated under a H_2/H_2S (15%) flow (6 L/h), at
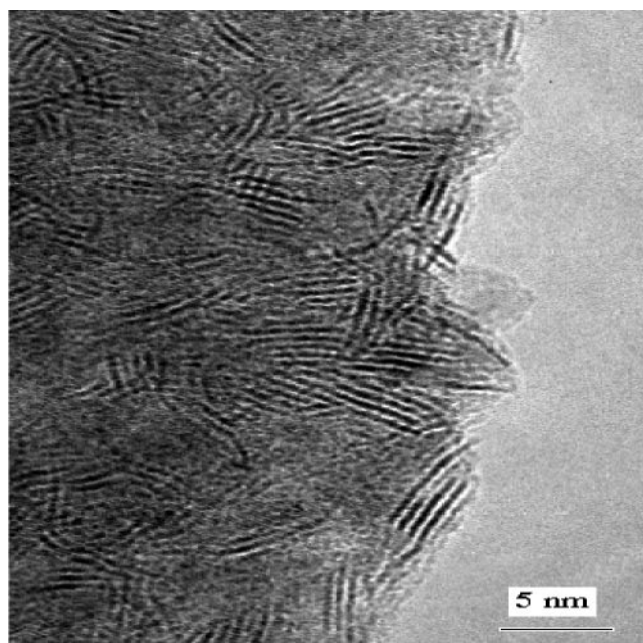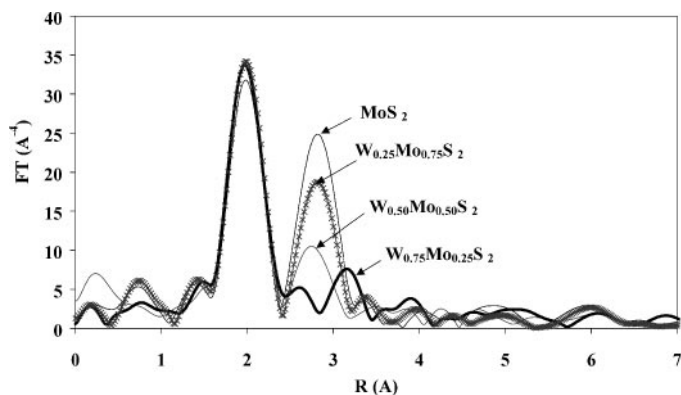

FIG. 3. TEM picture of $W_{0.50}Mo_{0.50}S_2$ sample prepared at 673 K by decomposition of the corresponding cocrystallized thiosalt ($G = 400,000$).

FIG. 4. Fourier transform obtained at the Mo K-edge for MoS_2 and $W_xMo_{(1-x)}S_2$ compounds prepared at 673 K by treatment, under H_2S flow, of mixed thiosalts resulting from cocrystallization of ammonium tetrathiotungstate and ammonium tetrathiomolybdate.

673 K, for 2 h, in order to obtain $W_xMo_{(1-x)}S_2$ compounds under the same conditions that make it possible to obtain WS_2 or MoS_2 from the corresponding thiosalts.

A sample with $x = 0.50$ was prepared in a similar way, but with a H_2/H_2S treatment carried out at higher temperature (1073 K instead of 673 K); it will be referred to as $W_{0.50}Mo_{0.50}S_2$-1073. Another sample ($x = 0.50$) was prepared at 673 K using a finely ground mixture of $(NH_4)_2WS_4$ and $(NH_4)_2MoS_4$ instead of the cocrystallization product obtained from the solution; it will be referred to as $W_{0.50}Mo_{0.50}S_2$-MM (MM = mechanical mixture).

Syntheses of the $W_xMo_{(1-x)}S_2$ compounds were also attempted from the two disulfides. WS_2 and MoS_2 were first obtained by a three-day reaction of sulfur with metal wires, in evacuated Pyrex or silica tubes, at 793 and 923 K, respectively. Mixtures of the two disulfides taken in the $x/(1-x)$ molar ratio were then carefully ground before firing at 823 K for one day and at either 1073 or 1273 K for one week and finally air-quenched or slowly cooled (4 K/h). These products will be referred to as $W_xMo_{(1-x)}S_2$-DM (DM = disulfide mixture).

We also prepared a $W_{0.50}Mo_{0.50}S_2$ sample by direct synthesis, i.e., reaction of sulfur on a mixture of fine Mo and W powders. The Pyrex tube was heated at 773 K for one week. After grinding, the resulting product was annealed in a silica tube at 1273 K for another week and finally slowly cooled. This compound will be referred to as $W_{0.50}Mo_{0.50}S_2$-DS (DS = direct synthesis).

III.2. X-Ray Diffraction Study

X-ray diffraction patterns of the samples prepared from the disulfides and by direct synthesis were recorded at the IMJR with an INEL CPS120-equipped powder diffractometer set up in a horizontal Debye–Scherrer geometry, using $CuK\alpha_1$ radiation (quartz monochromator).

XRD patterns of the samples obtained from thiosalts decomposition were recorded at the IRC using a Bruker D5005 diffractometer ($CuK\alpha_1$ radiation).

III.3. TEM-EDX Analysis

TEM analysis were performed with a HF 2000 Hitachi microscope (point-to-point resolution: 2.3 Å) working at 200 kV and equipped with a Kevex EDX detector with a Si–Li diode.

III.4. EXAFS Study

EXAFS spectra were recorded at the Laboratoire d'Utilisation du Rayonnement Electromagnétique (LURE), the French Synchrotron Laboratory, on the XAS 13 spectrometer, using a Si (111) monochromator for the tungsten L_{III} edge (10,100–11,200 eV, 2 eV step, 2 s per point, sum of three spectra) and a Ge (400) one for the molybdenum K-edge (19,800–21,000 eV, 4 eV step, 2 s per point, sum of three spectra). The storage ring (DCI) used 1.85-GeV positrons with an average intensity of 250 mA. For the sample preparation, pellets were pressed using quantities of powder calculated in order to achieve suitable absorption coefficient and edge jump. Data were collected in the transmission mode by measurement of the beam intensities I_0 and I, respectively, before and after passing through the sample, using ionization chambers.

Standard analysis of the EXAFS spectra (normalization, background removal, Fourier transformation, and curve fitting) were carried out using the SEDEM software (20) with FEFF (21) theoretical phase and amplitude functions. The curve-fitting procedure was performed in R-space. Fourier transformation of the normalized k^3-weighted EXAFS signal was performed over the k-range 2.5–16 Å^{-1} with Kaiser window functions. Coordination numbers (N), interatomic distances (R), Debye–Waller parameters (σ^2), and energy shifts (ΔE_0), were used as variables in the fitting procedure. Scale factors S_0^2 were fixed at 0.8.

IV. RESULTS AND DISCUSSION

IV.1. The $W_xMo_{(1-x)}S_2$ Compounds Obtained at 673 K from the Cocrystallized Thiosalts

The low temperature (673 K) used for the synthesis of the $W_xMo_{(1-x)}S_2$ ($x = 0.25, 0.50, 0.75$) compounds, and of the pure MoS_2 and WS_2 ($x = 0$ and 1), leads to poorly organized samples as demonstrated by the broadness of the X-ray diffraction lines (Fig. 2) and by the image of the small slabs with lattice fringes spacing of about 0.6 nm, characteristic of the MoS_2 (or WS_2) (002) basal plane (Fig. 3). It can nevertheless be seen that all the diffractograms correspond to the hexagonal cell of MoS_2 or WS_2. However, taking into account the important linewidth and the similarity of the
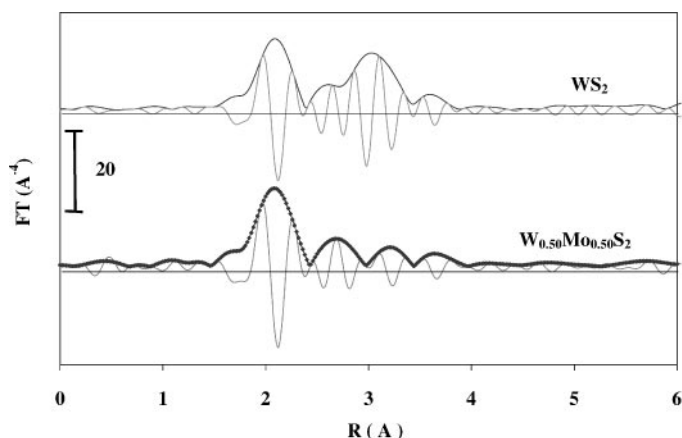
FIG. 5. Fourier transform obtained at the W L_{III}-edge for WS_2 and $W_{0.50}Mo_{0.50}S_2$ prepared at 673 K by treatment, under H_2S flow, of the mixed thiosalt resulting from cocrystallization of equimolar proportions of ammonium tetrathiotungstate and ammonium tetrathiomolybdate.

MoS_2 and WS_2 cell parameters, these data cannot make it possible to determine if the diffraction pattern of each of the mixed $W_xMo_{(1-x)}S_2$ compounds must be interpreted as a unique set of diffraction lines corresponding to the expected solid solution, or as the addition of the MoS_2 and WS_2 diagrams corresponding to a two-phase system. It will be seen below that EXAFS results unambiguously answer this question.

The first peak of the Fourier transform of the EXAFS spectra recorded either at the Mo K-edge (Fig. 4) or at the W L_{III} edge (Fig. 5) is fairly reproduced with ≈ 6 sulfur neighbors at a distance $d \approx 2.40$ Å, which corresponds to the expected anionic surrounding of the cations. Concerning now the cationic environment, it can be seen at the Mo K-edge (Fig. 4) that the Mo–Mo contribution (second peak) progressively decreases when the tungsten amount increases. For a high tungsten amount ($x = 0.75$), the cationic neighborhood signal is clearly split. This splitting can be related to the presence of a Mo–W contribution,

since Mo–W and Mo–Mo peaks have opposite phases: because of the resulting negative interference, the apparent peak positions are further apart than expected on the basis of the differences in distance and phase shift. In fact, this Mo–W contribution is already present for lower x values even if it does not clearly appear in the Fourier transform. Effectively (Table 1, Fig. 6), refinements of the EXAFS spectra show that the cationic in-plane environment of molybdenum contains both molybdenum and tungsten, with $N(W)/N(Mo)$ ratios compatible, taking into account the estimated error on the refined N values, with those involved in the synthesis. It thus appears that the $[MS_2]$ layers are heterocationic, according to the $[W_xMo_{(1-x)}S_2]$ formula.

A similar observation can be done at the W L_{III}-edge, as illustrated by Fig. 5, which allows the Fourier transforms obtained for WS_2 and $W_{0.50}Mo_{0.50}S_2$ (given as an example) to be compared. For $W_{0.50}Mo_{0.50}S_2$, the cationic environment signal is split into two peaks, due to the presence of W–Mo and W–W contributions (with opposite phases). It means again that every $[MS_2]$ layer contains molybdenum and tungsten. This is confirmed by the refinement of the EXAFS spectrum (Table 2, Fig. 7). It can thus be concluded that these compounds belong to a solid solution that involves heterocationic $[W_xMo_{(1-x)}S_2]$ layers, i.e., an intralayer solid solution.

IV.2. $W_{0.50}Mo_{0.50}S_2$-1073, the Compound Obtained at 1073 K from the Cocrystallized Thiosalts

EXAFS data make it possible to conclude that this compound is perfectly identical with those obtained at 673 K. The Fourier transforms are very similar and the fittings also make it possible to conclude that the cationic surrounding of each of the two cations is constituted by both molybdenum and tungsten neighbors (Table 3), in agreement with the existence of an intralayer solid solution. Therefore this new solid solid solution is thermally stable at least up to 1073 K.

TABLE 1

EXAFS Refinement Results (Mo K-edge): Characteristics of the Cationic In-plane Environment of Molybdenum in MoS_2 and $W_xMo_{(1-x)}S_2$ Compounds Prepared at 673 K by Treatment, under H_2S Flow, of Mixed Thiosalts Resulting from Cocrystallization of Ammonium Tetrathiotungstate and Ammonium Tetrathiomolybdate

	Mo shell				W shell			
	$R(Mo)$ (Å)	$N(Mo)$	$\sigma^2 \times 10^3$ (Å^2)	ΔE_0 (eV)	$R(W)$ (Å)	$N(W)$	$\sigma^2 \times 10^3$ (Å^2)	ΔE_0 (eV)
MoS_2	3.14	5.9	4.2	-1.6	—	—	—	—
$Mo_{0.75}W_{0.25}S_2$	3.15	4.5	4.0	2.8	3.15	1.9	8.8	5.8
$Mo_{0.5}W_{0.5}S_2$	3.16	3.2	4.5	2.4	3.17	2.1	4.7	6.9
$Mo_{0.25}W_{0.75}S_2$	3.16	2.3	3.5	2.0	3.15	4.8	4.2	-1.4

Note. The maximum errors estimated by the SEDEM software (20) are $\Delta R = \pm 0.02$ Å, $\Delta N = \pm 1$, $\Delta(\sigma^2) = \pm 10^{-3}$ Å^2, $\Delta(\Delta E_0) = \pm 1$ eV.
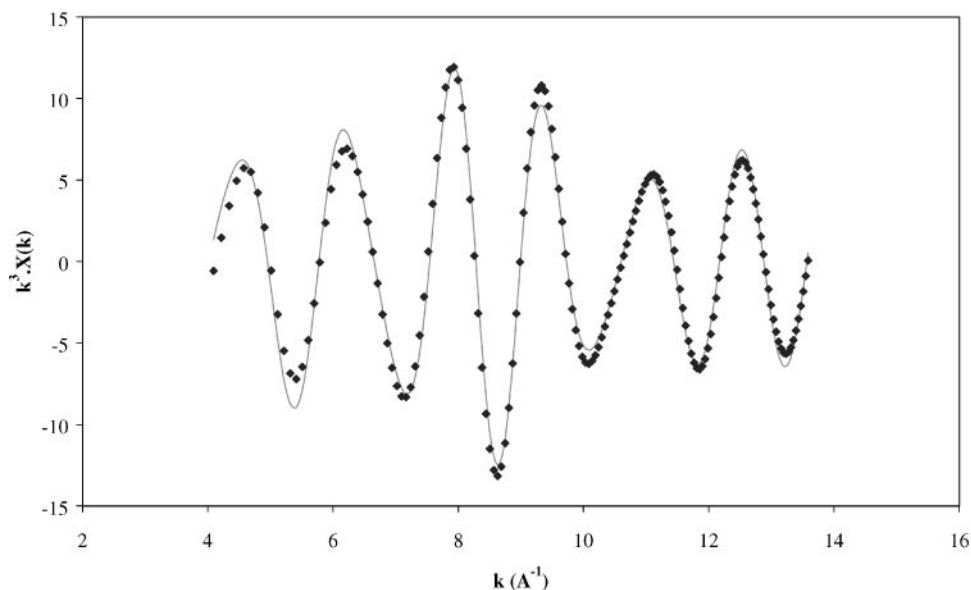
FIG. 6. Fourier-filtered EXAFS $k^3\chi(k)$ spectrum (diamonds) of the $W_{0.50}Mo_{0.50}S_2$ sample (cocrystallized thiosalt synthesis) fitted with a model Mo_{abs}–S–(Mo, W)–S (solid curve).

IV.3. $W_{0.50}Mo_{0.50}S_2$-MM, the Compound Obtained at 673 K from Mechanical Mixture of Ammonium Tetrathiomolybdate and Tetrathiotungstate

EXAFS study of this compound gives results significantly different from the previous ones. As shown by Fig. 8 (Mo K-edge), the second peak of the Fourier transform is perfectly the same for the mixed $W_{0.50}Mo_{0.50}S_2$-MM compound as for MoS_2. It means that molybdenum has only molybdenum in-plane cationic neighbors, and that tungsten has only tungsten in-plane cationic neighbors. This observation is confirmed by the refinement of the EXAFS spectrum (Table 3). It can thus be thought that this compound corresponds to an interlayer solid solution or to a two-phase system. EDX analyses performed with a 15–20 nm probe-size gave, as expected, a sulfur/metal atomic ratio close to 2, but for crystallites where molybdenum is present, no

significant amount of tungsten could be detected, and for crystallites where tungsten is present, no significant amount of molybdenum could be detected. It means that, in contrast to the cocrystallized thiosalts, mechanical mixture of ammonium thiomolybdate and thiotungstate leads to a mixture of the MoS_2 and WS_2 phases and is not a precursor that allows a solid solution to be obtained. This difference can be related to a higher segregation degree of the Mo and W cations in the mechanical mixture than in the cocrystallized thiosalts, whatever their precise nature, solid solution or intimate mixture.

IV.4. The $W_xMo_{(1-x)}S_2$-DM Samples Obtained at 1073 and 1273 K from the Disulfides

No notable difference could be detected in this series between quenched and slowly cooled samples of the same

TABLE 2

EXAFS Refinement Results (W L_{III}-edge): Characteristics of the Cationic In-plane Environment of Tungsten in WS_2 and $W_{0.50}Mo_{0.50}S_2$ Prepared at 673 K by Treatment, under H_2S Flow, of the Mixed Thiosalts Resulting from Cocrystallization of Equimolar Proportions of Ammonium Tetrathiotungstate and Ammonium Tetrathiomolybdate

	Mo shell				W shell			
	R(Mo) (Å)	N(Mo)	$\sigma^2 \times 10^3$ (Å^2)	ΔE_0 (eV)	R(W) (Å)	N(W)	$\sigma^2 \times 10^3$ (Å^2)	ΔE_0 (eV)
WS_2	—	—	—	—	3.15	3.9	1.7	8.8
$Mo_{0.5}W_{0.5}S_2$	3.18	2.8	1.66	15.4	3.16	3.5	2.0	9.9

Note. The maximum errors estimated by the SEDEM software (20) are $\Delta R = \pm 0.01$ Å, $\Delta N = \pm 0.6$, $\Delta(\sigma^2) = \pm 1.2 \times 10^{-3}$ Å^2, $\Delta(\Delta E_0) = \pm 1.4$ eV.
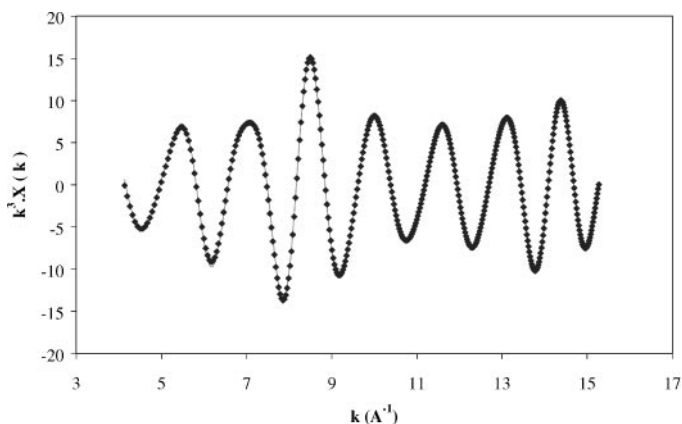
FIG. 7. Fourier-filtered EXAFS $k^3\chi(k)$ spectrum (diamonds) of the $W_{0.50}Mo_{0.50}S_2$ sample (cocrystallized thiosalt synthesis) fitted with a model W_{abs}–S–(Mo, W)–S (solid curve).
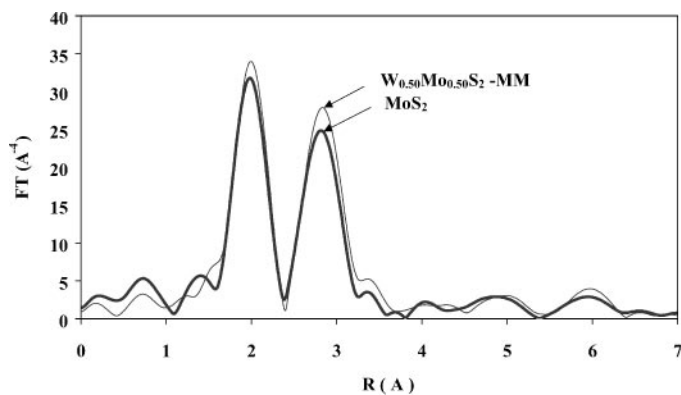
FIG. 8. Fourier transform obtained at the Mo K-edge for MoS_2 and $W_{0.50}Mo_{0.50}S_2$-MM prepared at 673 K by treatment, under H_2S flow, of a mechanical mixture of ammonium tetrathiotungstate and ammonium tetrathiomolybdate taken in equimolar proportions.

composition. These products are better crystallized than those obtained from the thiosalts, as evidenced by the TEM picture (Fig. 9), and cell parameters could be refined from X-ray diffraction data. No significant evolution of the a parameter vs. composition can be detected, which is not surprising since the a_{MoS_2} and a_{WS_2} parameters are nearly identical. As for the c parameter, it is found to increase with the tungsten content, which could indicate the occurence of a solid solution. However, despite the high synthesis temperature, the diffraction lines are broadened with respect to the instrumental linewidth and c_{MoS_2} and c_{WS_2} are not sufficiently different for the MoS_2 and WS_2 lines to be resolved in the diffraction pattern of a two-phase sample. This was verified using weighted additions of the experimental diffractograms of MoS_2 and WS_2 in order to simulate the diffractograms of two-phase $W_xMo_{1-x}S_2$ systems: no

splitting could be observed, even for the high angle 00l lines. Under these conditions, the c parameter evolution could result not from the existence of a solid solution, but from the use of a single-phase model for the refinement of the diffraction diagram of a two-phase system. At the MoK-edge, no significant difference can be observed between the FTs of the $W_{0.50}Mo_{0.50}S_2$ samples treated at 1073 and 1273 K, which are both similar to that of a well-crystallized MoS_2 sample (Fig. 10), as confirmed by the refined parameters (see Table 3). EDX analysis gives the same results as those obtained for the compound prepared from mechanical mixture of the thiosalts. It clearly means that, despite the high-temperature treatments, these samples contain distinct MoS_2 and WS_2 phases: even at temperatures as high as 1273 K, mixed $[W_{0.50}Mo_{0.50}S_2]$ layers cannot be obtained by reaction of preformed $[MoS_2]$ and $[WS_2]$ layers.

TABLE 3
EXAFS Refinement Results (Mo K-edge): Characteristics of the Cationic In-plane Environment of Molybdenum in Several $W_{0.50}Mo_{0.50}S_2$ Samples Prepared According to Different Methods

	Mo shell				W shell			
	$R(Mo)$ (Å)	$N(Mo)$	$\sigma^2 \times 10^3$ (Å^2)	ΔE_0 (eV)	$R(W)$ (Å)	$N(W)$	$\sigma^2 \times 10^3$ (Å^2)	ΔE_0 (eV)
$Mo_{0.5}W_{0.5}S_2$-673	3.16	3.2	4.5	2.4	3.17	2.1	4.7	6.9
$Mo_{0.5}W_{0.5}S_2$-1073	3.14	2.9	1.2	-0.3	3.13	3.4	3.0	-1.6
$Mo_{0.5}W_{0.5}S_2$-MM	3.16	5.4	3.1	2.5	—	—	—	—
$Mo_{0.5}W_{0.5}S_2$-DM-1073	3.15	6.4	2.3	2.5	—	—	—	—
$Mo_{0.5}W_{0.5}S_2$-DM-1273	3.13	5.6	3.2	-5.0	—	—	—	—
$Mo_{0.5}W_{0.5}S_2$-DS	3.14	3.3	1.0	-7.2	3.14	2.7	0.4	-6.4

Note. $W_{0.50}Mo_{0.50}S_2$-673 and $W_{0.50}Mo_{0.50}S_2$-1073 were prepared by treatment of the mixed thiosalt resulting from cocrystallization of equimolar proportions of ammonium tetrathiotungstate and ammonium tetrathiomolybdate, under H_2S flow, at 673 and 1073 K respectively. $W_{0.50}Mo_{0.50}S_2$-MM was prepared in a similar way at 673 K, but starting from a mechanical mixture of ammonium tetrathiotungstate and ammonium tetrathiomolybdate. $W_{0.50}Mo_{0.50}S_2$-DM-1073 and $W_{0.50}Mo_{0.50}S_2$-DM-1273 resulted from heating $WS_2 + MoS_2$ mixtures at 1073 and 1273 K, respectively. $W_{0.50}Mo_{0.50}S_2$-DS was obtained from reaction (1273 K) of sulfur on Mo + W powders.

The maximum errors estimated by the SEDEM software (20) are $\Delta R = \pm 0.01$ Å, $\Delta N = \pm 0.6$, $\Delta(\sigma^2) = \pm 0.4 \times 10^{-3}$ Å^2, $\Delta(\Delta E_0) = \pm 1$ eV.
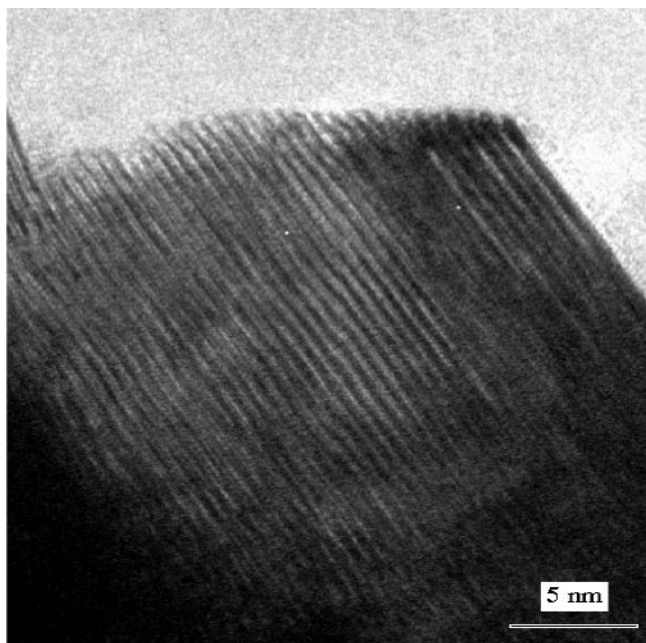
FIG. 9. TEM picture of the $W_{0.50}Mo_{0.50}S_2$ sample prepared from the disulfides at 1273 K ($G = 300,000$).

FIG. 10. Fourier transform obtained at the Mo K-edge for MoS_2 (crystallized at 1073 K) and two $W_{0.50}Mo_{0.50}S_2$ samples resulting from heating $WS_2 + MoS_2$ mixtures at 1073 and 1273 K.

IV.5. The $W_{0.50}Mo_{0.50}S_2$-DS Sample Obtained at 1273 K by Direct Synthesis ($W + Mo + S$)

As for the $W_xMo_{1-x}S_2$-DM products obtained from $MoS_2 + WS_2$, X-ray diffraction cannot determine the nature of the $W_{0.50}Mo_{0.50}S_2$-DS sample, whether it is a solid solution or mixture of WS_2 and MoS_2. EXAFS measurements at the Mo K-edge make it possible to answer this question since the cationic peak of the Fourier transform (Fig. 11) is clearly split, which is the signature of the
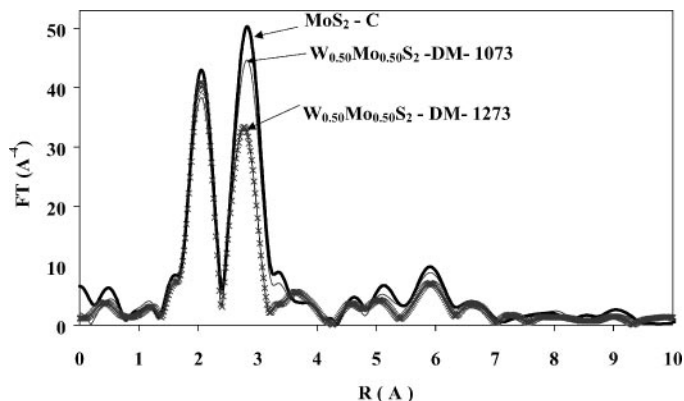
two-cation layers of the intralayer solid solution (Table 3). In the case of this synthesis route, it can then be thought that in the presence of sulfur, molybdenum, and tungsten powders directly react to form the mixed $[W_{0.50}Mo_{0.50}S_2]$ layers.

V. CONCLUSION

It must first be underlined that, using various synthesis conditions, we never observed formation of an interlayer solid solution. Even if the $[MoS_2]$ and $[WS_2]$ layers present quasi-identical in-plane periodicities, the intralayer solid solution appears more stable, as in the case of the Nb–Mo disulfide system. The geometrical factor cannot thus be considered as responsible for the obtention of the two-cation $[M_x^aM_{(1-x)}^bS_2]$ layers. Band structure calculations will be performed in order to identify the origin of the better
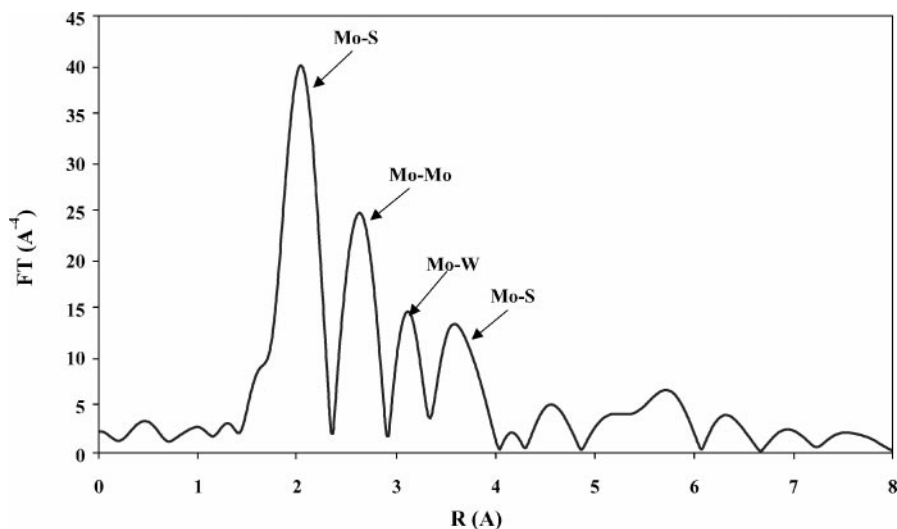

FIG. 11. Fourier transform obtained at the Mo K-edge for the $W_{0.50}Mo_{0.50}S_2$ sample prepared by direct synthesis.

stability of the intralayer model. Concerning now the intralayer solid solution, it appears that the synthesis temperature is not a decisive factor for its obtention. At temperatures as low as 673 K and starting from the cocrystallized thiosalts, the two-cation $[W_xMo_{(1-x)}S_2]$ layers of the intralayer solid solution are formed and are still stable at least up to 1073 K. However, up to 1273 K, no reaction between MoS_2 and WS_2, i.e., between already-existing $[MoS_2]$ and $[WS_2]$ layers, occurs. Starting from mechanical mixtures of the thiosalts does not lead to a solid solution either. These results show that the nature of the precursor is the decisive factor, and that the solid solution can be prepared only with a precursor in which the two cations are closely associated.

Lastly, this work demonstrates the power of EXAFS to characterize the structure of random 2-D compounds, something which would be practically impossible to do by diffraction methods.

REFERENCES

1. F. Hülliger, *in* "Structural Chemistry of Layered-Type Phases" (F. Lévy, Ed.). D. Reidel, Dordrecht, 1976.
2. H. Topsoe, B. S. Clausen, and F. E. Massoth, *in* "Catalysis Science and Technology, Vol. 11, Hydrotreating Catalysis" (J. R. Anderson and M. Boudart, Eds.). Springer-Verlag, Berlin, 1996.
3. I. L. Singer, *in* "Fundamentals in Friction: Macroscopic and Microscopic Processes" (I. L. Singer and H. M. Pollock, Eds.). Kluwer Academic, Dordrecht, 1992.
4. A. S. Golub, G. A. Protzenko, I. B. Shumilova, Ya. V. Zubavichus, C. Payen, Yu. N. Novikov, and M. Danot, *Mol. Cryst. Liq. Cryst.*, **311,** 377 (1998).
5. F. Kadijk, Thesis, University of Groningen, 1969.
6. V. Gaborit, Thesis, University of Nantes, 1998.
7. F. Wypych, K. Sollmann, and R. Schöllhorn, *Mater. Res. Bull.* **27,** 545 (1992).
8. B. K. Miremadi and S. R. Morrison, *J. Appl. Phys.* **67,** 1515 (1990).
9. C. Calais, N. Matsubayashi, C. Geantet, Y. Yoshimura, H. Shimada, A. Nishijima, M. Lacroix, and M. Breysse, *J. Catal.* **174,** 130 (1998).
10. W. J. Schutte, J. L. de Boer, and F. Jellinek, *J. Solid State Chem.* **70,** 207 (1987).
11. R. G. Dickinson and L. Pauling, *J. Am. Chem. Soc.* **45,** 1466 (1923).
12. K. D. Bronsema, J. L. de Boer, and F. Jellinek, *Z. Anorg. Allgem. Chem.* **540,** 15 (1986).
13. JCPDS files, 08-0237 and 37-1492.
14. M. Breysse, R. Fréty, M. Lacroix, and M. Vrinat, *React. Kinet. Catal. Lett.* **26,** 97 (1984).
15. E. Diemann and A. Müller, *Coord. Chem. Rev.* **10,** 79 (1973).
16. K. Ramanathan and S. W. Weller, *J. Catal.* **95,** 249 (1985).
17. G. Alonso, M. D. Valle, J. Cruz, V. Petranovskii, A. Licea-Claverie, and S. Fuentes, *Catal. Today* **43,** 117 (1998).
18. P. Belougne, N. Chézeau, and J. Lapasset, *Acta Crystallogr. Sect. B* **32,** 3087 (1976).
19. K. Sasvari, *Acta Crystallogr.* **16,** 719–724 (1963).
20. D. Aberdam, *J. Synchrotron Rad.* **5,** 1287–1297 (1998).
21. J. J. Rehr, S. I. Zabinsky, and R. C. Albers, *Phys. Rev. Lett.* **69,** 3397 (1992).